Second-order nonlinear optical properties of stilbene, benzylideneaniline and azobenzene derivatives. The effect of π-bridge nitrogen insertion on the first hyperpolarizability

Cornelis A. van Walree,[a] Okke Franssen,[a] Albert W. Marsman,[a] Marinus C. Flipse[b] and Leonardus W. Jenneskens*,[a]

[a] *Debye Institute, Department of Physical Organic Chemistry, Utrecht University, Padualaan 8, 3584 CH Utrecht, The Netherlands*
[b] *Akzo Nobel Central Research, PO Box 9300, 6800 SB Arnhem, The Netherlands*

The second-order nonlinear optical (NLO) and electronic properties of stilbenes (C=C bridge), benzylideneanilines (C=N and N=C bridges) and azobenzenes (N=N bridge) containing either an *N*,*N*-dimethylamino donor and/or a nitro acceptor were investigated using EFISH, UV spectroscopy, cyclic voltammetry and PPP/SCF calculations. It appeared that although first hyperpolarizabilities of the ethylene and azo bridged donor–acceptor compounds are of comparable magnitude, substitution of one carbon by a nitrogen atom reduces the NLO activity. Differences in hyperpolarizabilities were rationalized with the aid of a two-level model, which revealed that they find their origin in the redox activity of the nitrogen-containing bridges.

Introduction

On account of possible application in photonic materials and devices the second-order nonlinear optical (NLO) properties of organic substances have been intensively investigated over the past decades.[1–5] In particular the microscopic second-order nonlinear optical coefficients or (first) hyperpolarizabilities β of donor–acceptor substituted π-conjugated (DπA) compounds are promising, as these compounds dispose of a low-lying charge-separated first excited state. While considerable progress has been made in the understanding and development of structure–activity relationships for DπA compounds,[6–10] much work remains to be done in order to understand effects of specific structural modifications on nonlinear optical properties. One of these topics is the effect of incorporation of nitrogen in the π-conjugated bridge. Although this issue has been treated in several computational studies[11–14] a detailed experimental study has hitherto not been reported. The point has been addressed in an experimental study,[15] but only laterally and results were somewhat complicated because of the use of different substituents. Therefore, in the present study the second-order nonlinear optical properties of *N*,*N*-dimethylamino and/or nitro substituted stilbenes (compound type **1**), benzylideneanilines (compound types **2** and **3**) and azobenzenes (compound type **4**) are discussed (Scheme 1). In addition, electronic transitions and redox potentials, being of interest for the understanding of interactions between the substituents and the bridges and hence hyperpolarizabilities are evaluated. In order to interpret the experimental data they are considered along with results of PPP/SCF and PM3 semi-empirical calculations.

It should be realized at the outset that the molecular geometries of the benzylideneanilines, with the exception of **2DA**, are not planar. The phenylene groups linked to the azomethine nitrogen atom can be severely twisted from the C–N=C–C plane,[3,14,16–21] through which electronic and nonlinear optical properties can be considerably affected. This subject is further elaborated in the accompanying paper.[22] Molecular structures of stilbene and azobenzene derivatives are thought to be essentially planar.[14,23,24]

Results and discussion

Redox potentials

In order to gain insight into the response of frontier orbitals to nitrogen incorporation oxidation and reduction potentials E_{ox} and E_{red} were determined by cyclic voltammetry. In the donor substituted series **1**–**4D** oxidation potentials range from +0.41 V for **1D** to +0.80 V for **4D** (Table 1). The differences can be rationalized by considering the orbital energies of the parent compounds **1**–**4**, such as calculated with the PPP/SCF method[25,26] (Table 2, Fig. 1). The HOMOs of **1**–**4D** are formed by a linear combination of the HOMOs of **1**–**4** and a high energy filled orbital supplied by the dimethylamino substituent.[27,28] Since the HOMO of stilbene **1** is situated at the highest energy the interaction of this orbital with the dimethylamino group will be the most favourable, which leads to the highest energy for the resulting orbital of **1D**. In other words, the low oxidation potential of **1D** reflects the high energy of the stilbene HOMO. Likewise the highest oxidation potential is obtained for azobenzene **4D**, as the azobenzene HOMO possesses the lowest energy. Oxidation potentials of benzylideneanilines **2D** and **3D** are situated between those of **1D** and **4D**; their magnitudes are however considerably affected by the position of the nitrogen atom in the azomethine bridge (*vide infra*).

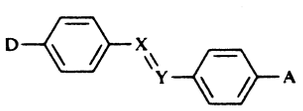

	X=Y		D	A
1	HC=CH	**1–4**	H	H
2	N=CH	**1–4D**	Me_2N	H
3	HC=N	**1–4A**	H	NO_2
4	N=N	**1–4DA**	Me_2N	NO_2

Scheme 1

It is worthwhile to compare the oxidation potentials of **1**–**4D** with that of *N*,*N*-dimethylaniline, +0.64 V *vs.* SCE. The lower potential of stilbene **1D** can be attributed to the extension of the π-system, while the increase found for **4D** is caused by the electron-accepting ability of the azo bridge, which counteracts the electron-donating behaviour of the dimethylamino donor. When in the benzylideneanilines the nitrogen atom is positioned at the side of the dimethylamino group (**2D**) E_{ox} is lowered compared to that of *N*,*N*-dimethylaniline; the bridge thus reinforces the electron-donating ability of the donor. The oxidation potential of **3D**, on the contrary, is almost as high as

Table 1 Oxidation and reduction potentials, relative to SCE, of compound series **1**–**4D**, **1**–**4A** and **1**–**4DA**

	E_{ox}/V	E_{red}/V		E_{ox}/V	E_{red}/V
1D	+0.41	**1A** −1.20	**1DA**	+0.49	−1.21
2D	+0.58	**2A** −1.08	**2DA**	+0.63	−1.10
3D	+0.76	**3A** −1.20	**3DA**	+0.85	−1.23
4D	+0.80	**4A** −0.95	**4DA**	+0.86	−1.03

Table 2 PPP/SCF calculated orbital energies of frontier molecular orbitals of compounds **1**–**4**, **1**–**4D**, **1**–**4A** and **1**–**4DA**

	E_{HOMO}/eV	E_{LUMO}/eV		E_{HOMO}/eV	E_{LUMO}/eV
1	−9.05	−2.14	**1A**	−9.29	−2.84
2(3)	−9.20	−2.51	**2A**	−9.40	−3.13
4	−9.56	−3.09	**3A**	−9.49	−2.94
1D	−7.76	−1.67	**4A**	−9.80	−3.47
2D	−7.64	−2.08	**1DA**	−7.90	−2.57
3D	−8.01	−1.96	**2DA**	−7.78	−2.82
4D	−8.00	−2.56	**3DA**	−8.18	−2.53
			4DA	−8.16	−2.99

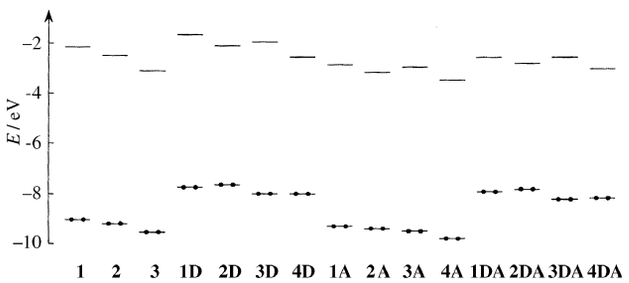

Fig. 1 PPP/SCF calculated HOMO and LUMO energies of compound series **1**–**4**, **1**–**4D**, **1**–**4A** and **1**–**4DA**

that of azobenzene **4D**, indicating electron-accepting behaviour of the bridge.

Reduction potentials of πA systems **1**–**4A** do not vary as pronouncedly as the oxidation potentials of the Dπ systems **1**–**4D**. They all are weakly to moderately lowered with respect to the potential of nitrobenzene (−1.25 V *vs.* SCE). The sequence in reduction potential in the series **1**–**4A** appears to be dictated by the LUMO energies of the unsubstituted compounds. Thus, the reduction potentials **1A** and **4A** mirror the oxidation potentials of their donor substituted analogues. The low oxidation potential of **1D** is accompanied by a high reduction potential of **1A**, and the high oxidation potential of **4D** is connected with the low reduction potential of **4A**, again reflecting the electron-accepting ability of the azo bridge. Such a relation is however not found for benzylideneanilines **2A** and **3A**. The azomethine bridge in compounds of type **2** substantially lowers the acceptor reduction potential, whereas it was also found to lower the donor oxidation potential. Simultaneously the electron-accepting character of the bridge in **3D**, as indicated by its high oxidation potential, is not reflected in a low reduction potential of **3A**. This behaviour can be attributed to polarization of the azomethine bridge through which the nitrogen atom is partially negatively charged and the carbon atom is partially positively charged.[14] The HOMO of *N*,*N*-dimethylaniline is therefore destabilized by the adjacent nitrogen atom in **2D** and stabilized by the adjacent carbon atom in **3D**. On the other hand, reduction of the nitrophenyl moiety is more facilitated by the neighbouring positive carbon atom than when linked to the negative nitrogen atom. These observations are in line with findings by El-Aasser *et al.*[29]

It is important to note that redox potentials of planar analogues of the benzylideneanilines are almost equal to those given in Table 1.[22] Hence, the potentials appear to be rather independent of the molecular conformation. This provides evidence that an interaction between the lone pair on the azomethine nitrogen atom and the π-systems in non-planar geometries is not of interest for the redox potentials. Moreover the similarity in potentials of planar and twisted derivatives indicates that π-conjugation has a minor influence on the redox potentials and confirms that the redox potentials are primarily determined by the polarization of the C=N bond. The differences in redox potentials are also in line with the small dipole moments[30,31] of **2D** and **2A** relative to those of **3D** and **3A** (*vide infra*, Table 5). As a result of the polarization of the azomethine bridge the charges induced by the substituents remain localized in the phenyl groups in **2D** and **2A** and are more transported towards the bridge in **3D** and **3A**.

Trends in oxidation and reduction potentials of the donor–acceptor compounds **1**–**4DA** are similar to those found for their reference compounds containing only a donor or acceptor group. However, both oxidation and reduction potentials are systematically higher than the potentials of **1**–**4D** and **1**–**4A**, respectively. These changes originate from mixing of donor and acceptor orbitals and reflect their ground state interactions.

The experimental redox potentials are confirmed by the PPP/SCF energy levels (Table 2, Fig. 1).†‡ Trends in HOMO and LUMO energies are satisfactorily reproduced, with the exception of the HOMOs of **2D** and **2DA**. It may well be that the destabilizing effect of the azomethine nitrogen atom on the HOMO of these compounds is overestimated. Nevertheless, the calculated energy levels support our finding that the orientation of the bridge such as in compound type **2** leads to increased electron-donating and -accepting abilities of the respective dimethylamino and nitro groups, and that the orientation of the bridge in compounds of type **3** results in a stronger delocalization of substituent effects over the π-system. Note that the position of orbitals relative to the HOMO of *N*,*N*-dimethylaniline (−7.92 eV) and the LUMO of nitrobenzene (−2.63 eV) is fully in line with the redox potentials.

Electronic transitions

The characteristics of the electronic transitions of the compounds under investigation are compiled in Table 3. Absorption maxima and the composition of transitions according to configuration interaction (CI) such as calculated by the PPP/SCF method are recorded as well. In order to facilitate comparison of the theoretical (gas phase) data with experimental data absorption maxima in cyclohexane (ν_{chx}) are added. Although the gas phase PPP transition energies are generally hypsochromically shifted trends are consistent with those in the experimental data. Trends in calculated transition intensities proved to be unreliable; therefore calculated intensities are not taken into consideration.

For the parent compounds **1**–**4** the UV bands of interest are the π–π* bands situated at 31 300 to 33 600 cm^{-1}. These bands shift bathochromically upon incorporation of either one or two nitrogen atoms in the bridge. Fig. 1 reveals that although substitution of a C–H bridge unit by a nitrogen atom lowers both the HOMO and LUMO, the stabilizing effect on the latter is stronger, which accounts for the bathochromic shift.[27] The spectrum of **2** (**3**) is however complicated because of the non-planar geometry of this compound and the fact that several bands overlap.[16,19,27,33] It is therefore more appropriate to consider the electronic absorption spectrum of 2-phenyl-3,3-dimethyl-3*H*-indole, a planar model compound of **2** (ν_{max} = 32 400 cm^{-1}, ε_{max} = 17 000 dm^3 mol^{-1} cm^{-1}).[19] UV spectra of substituted benzylideneanilines can also suffer from non-planar molecular

† Although the PPP/SCF method is a π-electron method it treats σ-electron effects *via* the parametrization.[26,32] Consequently, in the PPP/SCF calculations the polarization of the azomethine bridge, which occurs in the σ-framework, is implicitly taken into account.

‡ The changes in both oxidation and reduction potentials upon incorporation of nitrogen atoms in the bridge are also in agreement with *ab initio* calculated energy levels of donor–acceptor-substituted nitrogen containing polyenes.[13]

Table 3 UV–VIS properties of compounds **1–4**, **1–4D**, **1–4A** and **1–4DA**

	$\nu_{max}/10^3$ cm^{-1}	$\varepsilon_{max}/10^3$ dm^3 mol^{-1} cm^{-1}	μ_{ge}/D [a]	$\nu_{chx}/10^3$ cm^{-1}	$\nu_{calc}/10^3$ cm^{-1} [b]	χ_{H-L} [c]	χ_{H-L+1} [d]
1	33.6	25.7	6.55	33.8	33.2	0.99	
2(3)	32.1	7.8	3.70	31.7	31.3	0.99	
4	31.3	19.4	5.27	31.6	29.1	0.99	
1D	28.3	31.5	6.40	28.8	29.5	0.97	
2D	26.6	13.8	4.72	26.5	26.0	0.97	
3D	28.3	31.0	6.34	29.3	28.4	0.97	
4D	24.4	31.1	7.29	25.0	24.9	0.98	
1A	28.4	22.0	6.36	29.3	32.1	0.95	0.22
2A	28.8	10.4	4.54	29.1	30.5	0.94	−0.28
3A	30.2	17.8	5.48	30.9	31.2	0.98	
4A	29.9	21.3	6.23	30.3	29.3	0.98	
1DA	22.9	27.1	6.94	24.0	26.5	0.86	0.41
2DA	22.0	19.9	6.10	22.9	23.6	0.90	−0.36
3DA	24.9	28.2	7.00	26.3	26.6	0.88	0.36
4DA	20.9	29.5	7.22	22.4	23.6	0.94	0.23

[a] Transition dipole moment in chloroform; 1 D = 3.336 × 10^{-30} C m. [b] PPP calculated absorption maximum. [c] HOMO ⟶ LUMO configuration interaction vector. [d] HOMO ⟶ LUMO + 1 configuration interaction vector.

conformations and band overlap.[33] Nevertheless, observed trends for the benzylideneanilines are similar as found for their planar analogues, the 2-phenyl-3,3-dimethyl-3*H*-indoles,[19,22,33] indicating that they are related to intrinsic electronic properties. Moreover, according to our PPP/SCF CI data the lowest energy bands of the parent and monosubstituted benzylideneanilines correspond to the HOMO–LUMO transition. This implies that the UV data of the benzylideneanilines are mutually consistent and enables comparison of the spectra of the benzylideneanilines with those of the stilbenes and azobenzenes since the frontier orbitals of all compound classes are essentially similarly shaped (Fig. 2). It should furthermore be noted that in the spectra of compounds **2** (**3**) and **4** n–π* transitions are present at *ca.* 28 000 (**2**, ε_{max} = 60 dm^3 mol^{-1} cm^{-1}) and 22 600 cm^{-1} (**4**, ε_{max} = 500 dm^3 mol^{-1} cm^{-1}). These bands are often submerged under the π–π* bands in the substituted compounds and are of negligible interest because of their small intensities.

The UV bands of compounds **1–4D** can be interpreted as π–π* bands with charge transfer (CT) character. Taking the MOs depicted in Fig. 2 as being indicative, it is seen that upon HOMO–LUMO excitation charge is transferred from the dimethylamino group towards the π-systems. When going from **1D** to **4D**, *i.e.* with increasing oxidation potential, charge transfer is gradually more favoured to the bridge instead of to the unsubstituted phenyl group. The positions of the UV bands are thus related to the donor oxidation potential and the electron-accepting ability of the bridge. This is confirmed by the PPP calculated energy levels and transition energies.

The low intensity of the UV band of **2D** is remarkable. It was seen above that the negatively charged nitrogen in the azomethine bridge obstructs the donation of electron density from the dimethylamino group to the bridge. This also rationalizes the transition dipole moment μ_{ge}, which corresponds to the shift of charge during an electronic transition, is small.

The UV spectra of the nitro compounds **1–4A** are less convincingly related to redox potentials and orbital energies. As a consequence the PPP/SCF/CI calculations do not give the correct order of transition energies. However, differences between both experimental and theoretical UV maxima of the nitro compounds are relatively minor, and small errors in the calculated data rapidly lead to a reversion of order in transition energies. The transitions are accompanied by CT from the unsubstituted phenyl rings to the nitro groups, but for **3A** and **4A** CT seems to occur preferentially to the bridge, rather than to the nitro groups (Fig. 2). The small transition intensity of **2A** can be rationalized by using the same argument as was used to explain the small intensity of the lowest transition of **2D**.

The spectra of the donor–acceptor substituted compounds

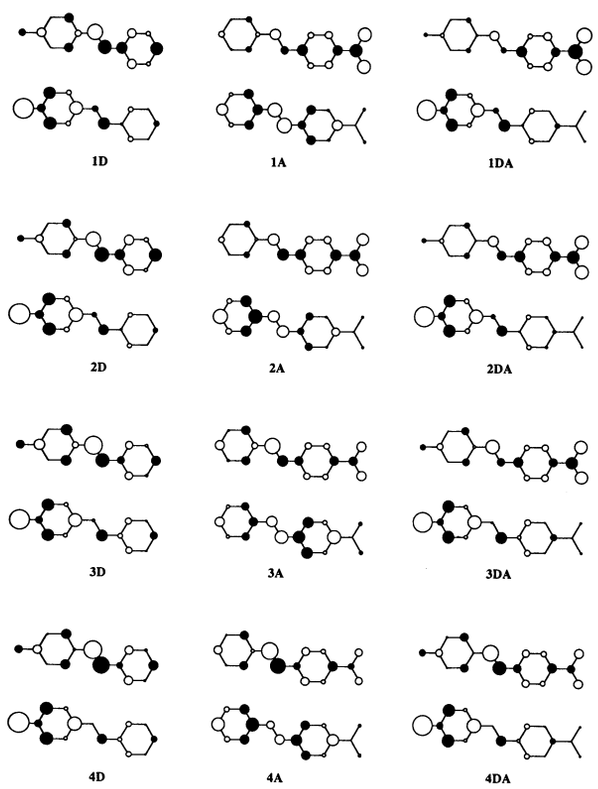

Fig. 2 PPP/SCF calculated HOMOs (bottom) and LUMOs (top) of compound series **1–4D**, **1–4A** and **1–4DA**

1–4DA are dominated by their intense CT bands. As is generally known and illustrated in Fig. 2 these bands are mainly based on promotion of an electron from a HOMO corresponding to those of donor compounds **1–4D** to a LUMO similar to that of the nitro compounds **1–4A**. The maxima of the CT bands however do not correlate with the differences in redox potentials.§

§ Although this may be attributed to the involvement of differing repulsion and exchange integrals, the differences in redox potentials already deviate from the PPP calculated HOMO–LUMO gaps, which lead to reasonable calculated transition energies (Tables 2 and 3) when two facts are taken into account. The first one is that planar molecular geometries were used in the calculations, while **3DA** is definitely not planar.[17,18,20,33] Since the (experimental) absorption maximum of **3DA** is blue shifted relative to that of the analogously substituted 3*H*-indole[22,33] the PPP calculated transition energy is underestimated. The second one is that the HOMO of **2DA** is calculated to lie at a too high energy, and ν_{calc} of this compound should thus be somewhat higher.

Table 4 Fluorescence solvatochromism of donor–acceptor substituted compounds

		1DA		2DA		3DA	
Solvent	Δf	$\nu_{abs}/10^3$ cm^{-1}	$\nu_{fl}/10^3$ cm^{-1}	$\nu_{abs}/10^3$ cm^{-1}	$\nu_{fl}/10^3$ cm^{-1}	$\nu_{abs}/10^3$ cm^{-1}	$\nu_{fl}/10^3$ cm^{-1}
Cyclohexane	−0.002	24.0	20.0	22.9	19.9	26.3	21.4
Dibutyl ether	0.096	23.9	18.1	22.9	18.4	25.9	20.1
Diethyl ether	0.162	23.8	16.8	22.9	16.9	25.8	19.0
Ethyl acetate	0.200	23.5	15.0	22.7	15.1	25.4	17.1
THF	0.210	23.1	14.9	22.4	15.2	25.0	16.7
Acetonitrile	0.305	23.3	*a*	22.6	*a*	25.0	*a*
$C/10^3$ cm^{-1}		3.91		2.77		4.52	
$2\Delta\mu^2/hc\rho^3/10^3$ cm^{-1}		20.90		21.45		17.80	
r^b		0.991		0.983		0.978	
$\Delta\mu$/D		16.6		16.8		15.3	
μ_e/D ^{c}		24.0		23.7		23.9	
$\Delta\mu_{ec}$/D ^{d}		19		16		15	

^{a} No fluorescence observed. ^{b} Correlation coefficient. ^{c} Excited state dipole moment using μ_g data given in Table 5. ^{d} $\Delta\mu$ determined by absorption electrochromism.[37]

It is noteworthy that for an adequate theoretical description of the CT transitions configuration interaction is important, particularly for the stilbene and the benzylideneanilines.¶ The CI vectors show that the HOMO–SLUMO transition is of interest as well. In all donor–acceptor compounds this SLUMO is mainly localized on the nitro groups and the bridges. The participation of a third state in the optical transitions imposes questions upon the validity of the two-level model for the description of the hyperpolarizabilities of these compounds (*vide infra*).

The CT bands are generally more intense than the bands found in the unsubstituted or monosubstituted compounds. This observation is explained by the greater delocalization of the excited electron in the donor–acceptor substituted compounds during the transition. This is particularly evident for the intensities of the benzylideneanilines of type **2**. Nevertheless the transition dipole moment μ_{ge} of **2DA** is still small compared to those of the other donor–acceptor substituted compounds, suggesting that the nature of the bridge is the principal factor of interest for the intensity of the absorptions.

The two-level model

For donor–acceptor substituted compounds the static (frequency independent) CT contribution to the first hyperpolarizability, $\beta_{CT}(0)$, can be determined by use of eqn. (1), in which μ_{ge}

$$\beta_{CT}(0) = \frac{\mu_{ge}^2 \Delta\mu}{E^2} \quad (1)$$

is the transition dipole moment (in D) of the electronic transition of energy E ($E = h\omega_{max}$, h being the Planck constant and ω_{max} the frequency at maximum absorption) and $\Delta\mu$ (D) is the difference between the excited and ground state static dipole moments. This model predicts that large first hyperpolarizabilities are obtained for compounds undergoing a large change in static dipole moment upon excitation and possessing an intensive and low energy CT transition. The transition dipole moment μ_{ge} is obtained from the oscillator strength f of a transition, eqn. (2), with $3he^2/8\pi^2 m_e = 7.095 \times 10^{-43}$ C^2 m^2 s^{-1}. The

$$|\mu_{ge}|^2 = \frac{3he^2 f}{8\pi^2 m_e \omega_{max}} \quad (2)$$

oscillator strength is calculated with eqn. (3), where ε_{max} is the

$$f = 4.32 \times 10^{-9}\, \varepsilon_{max} \Delta\nu_{\frac{1}{2}} \quad (3)$$

extinction coefficient at the absorption maximum and $\Delta\nu_{\frac{1}{2}}$ the band width at half height, preferably determined at the red side of the band.

The difference in dipole moment $\Delta\mu$ can be derived from fluorescence solvatochromism of donor–acceptor systems[34] eqns. (4).

$$\nu_{abs} - \nu_{fl} = C + \frac{2\Delta\mu^2}{hc\rho^3}\Delta f \quad (4a)$$

$$\text{with } \Delta f = \frac{\varepsilon_s - 1}{2\varepsilon_s + 1} - \frac{n^2 - 1}{2n^2 + 1} \quad (4b)$$

In these equations ν_{abs} and ν_{fl} represent the absorption and emission wavenumber, respectively (Table 4), C a constant, c the speed of light and ρ the effective radius of the solute. The solvent polarity parameter Δf is related to the solvent relative permittivity ε_s and refractive index n.‖ By plotting $\nu_{abs} - \nu_{fl}$ *vs.* Δf, $\Delta\mu$ can be obtained from the slope of the linear fit provided that ρ, which is of critical importance for the magnitude of $\Delta\mu$, is known. There are several approaches to estimate this parameter.[36] For the compounds under investigation it is most appropriate to assume a cylindrical symmetry and calculate the radius from the length L and diameter D of the cylinder, eqn. (5).

$$\rho = (\tfrac{3}{16} L D^2)^{1/3} \quad (5)$$

Using lengths (16.5 Å) and diameters (6.6 Å) derived from CPK models a radius of 5.1 Å for all donor–acceptor substituted compounds is obtained. Resulting $\Delta\mu$ values, compiled in Table 4, are in good agreement with those determined by electrochromic absorption and fluorescence measurements.[37]

The solvatochromism method is not applicable to the nonfluorescent azobenzene **4DA**. Although it has been claimed that absorption solvatochromism can be used to evaluate $\Delta\mu$[38] and hence $\beta_{CT}(0)$,[39] we consider this method unreliable. It is for instance seen in Table 4 that absorption solvatochromism is much more pronounced for **3DA** than for **2DA**, while fluorescence solvatochromic sensitivities $2\Delta\mu^2/hc\rho^3$ are of comparable magnitude. Moreover, application of absorption solvatochromism has led to some unreasonable estimates for excited state dipole moments of donor–acceptor substituted benzylideneanilines.[40] Thus, rather than to rely upon absorption solvatochromism we use for $\Delta\mu$ of **4DA** the literature value[37] of 17.0 D, determined by electrochromic absorption measurements,

¶ Without configuration interaction the transitions are calculated to occur at 28 800 (**1DA**), 25 400 (**2DA**), 29 000 (**3DA**) and 24 900 (**4DA**) cm^{-1}, *i.e.* considerably hypsochromically shifted.

‖ Relative permittivity and refractive indices of solvents were taken from Reichardt.[35]

Table 5 PM3 calculated vector components of ground state dipole moments and first hyperpolarizabilities of **1–4D**, **1–4A** and **1–4DA**

	μ_x/D	μ_y/D	$\lvert\mu_z\rvert$/D [a]	μ_{calc}/D	μ_g/D [b]	β_x/au [c]	β_y/au [c]	$\lvert\beta_z\rvert$/au [a,c]	$\beta_{tot}/10^{-30}$ esu [d]	$\beta_\mu/10^{-30}$ esu [e]	θ_{xy}/° [f]
2,3	0.30	1.23	0.01	1.25	1.6	240	41	1	2.1	−0.8	67
1D	1.07	0.05	0.91	1.41	2.4	1563	118	123	13.6	9.4	2
2D	1.42	1.17	0.90	2.04	2.7	1227	−127	114	10.7	6.3	45
3D	−0.78	1.27	0.94	1.77	3.6	−1921	88	117	16.6	7.3	56
4D	2.26	0.15	0.72	2.38	3.2	1649	133	167	14.4	11.0	1
1A	6.36	0.28	0.02	6.37	4.6	1524	226	5	13.3	13.3	6
2A	6.52	0.99	0.01	6.60	4.2	789	−132	0	6.9	6.6	18
3A	−5.96	1.45	0.01	6.13	5.0	−1392	52	1	12.0	11.8	12
4A	6.15	0.23	0.02	6.15	4.5	833	60	8	7.2	7.2	2
1DA	7.69	0.38	0.92	7.75	7.4	4322	407	134	37.5	37.1	3
2DA	7.91	0.74	0.92	8.00	6.9	3212	−409	128	28.0	26.6	13
3DA	−7.30	1.96	0.94	7.62	8.6	−4231	437	127	36.8	36.3	9
4DA	7.68	0.22	0.88	7.73	8.2	3487	179	138	30.2	29.9	1

[a] Absolute values are given since inversion of the configuration at nitrogen can occur. [b] Experimental (ground state) dipole moment taken from literature.[31] Dipole moments were measured in benzene at 25 °C; for all benzylideneanilines the temperature was not specified.[30] [c] 1 au = 8.641×10^{-33} esu. [d] Calculated total hyperpolarizability in units of 10^{-30} esu; 1 esu = 1 cm^5 s C^{-1} = 3.71×10^{-21} C^3 m^3 J^{-2}. [e] Calculated projection of the hyperpolarizability along the dipole moment in units of 10^{-30} esu. [f] Angle between dipole moment and hyperpolarizability vectors in the *xy* plane.

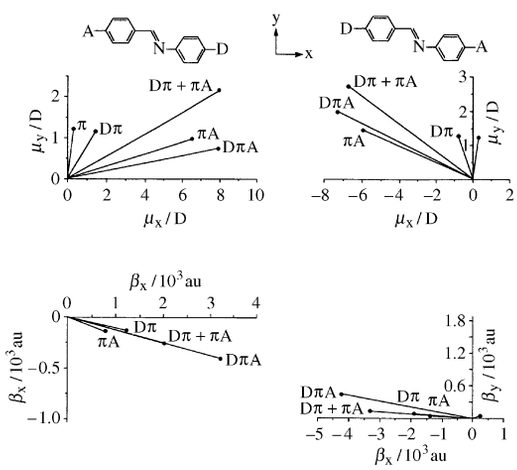

Fig. 3 Schematic representation of PM3 calculated dipole moment and first hyperpolarizability vector components of benzylideneanilines of type **2** (left) and **3** (right) in the given molecular orientations. In order to show more detail, represented angles θ_{xy} do not correspond to actual calculated angles (see Table 5).

from which it follows that the excited state dipole moment μ_e is 25.2 D.

The data in Table 4 reveal that the $\Delta\mu$ values of **1–4DA** are of comparable magnitude. Excited state dipole moments μ_e are virtually independent of the nature of the bridge and appear to be determined by the donor–acceptor combination only, despite the fact that the PPP calculations reveal a substantial electron density at the bridge in the LUMOs of **3DA** and **4DA**. The two-level hyperpolarizability $\beta_{CT}(0)$ of the azobenzene **4DA** is the largest, followed by those of **1DA** and the two benzylideneanilines, of which $\beta_{CT}(0)$ is of similar magnitude (see Table 7). Nitro compounds **1–4A** are non-fluorescent and the fluorescence of dimethylamino compounds **1–4D** is, if present, only very weakly solvatochromic, which thwarts determination of $\beta_{CT}(0)$ of these monosubstituted compounds.

First hyperpolarizabilities β

Hyperpolarizabilities were determined with the electric field-induced second-harmonic generation (EFISH) technique. The alternative hyper-Rayleigh scattering (HRS) technique is not suitable for some of the compounds under investigation, since we have recently shown that two-photon absorption followed by fluorescence near the second-harmonic wavelength occurs.[41,42] Ground state dipole moments μ_g, required since the EFISH method gives the scalar product $\beta\mu_g$, were taken from literature.[31] Though it is often assumed that β and μ are oriented in the same direction, this is not the case for the monosubstituted benzylideneanilines. This is illustrated by calculation of the vector components of dipole moments and hyperpolarizabilities by a finite field method using the PM3 parametrization of the MNDO hamiltonian (Table 5, Fig. 3).**[,43,44] The results of these calculations show that the azomethine bridge possesses a non-negligible dipole moment, which, according to its direction, seems to be associated to the presence of the electron lone pair at the nitrogen atom. The dipole moment of the bridge has a profound effect on the direction of the small dipole moments of compounds **2D** and **3D**, which accordingly deviate strongly from the CT axis along which the hyperpolarizabilities are directed. Another factor which causes the dipole moments of **1–4D** to deviate from the CT axis is a dipole component along the *z*-axis, which is caused by the calculated position of the dimethylamino group out of the plane of the adjacent phenylene group. However, as shown before[24] the PM3 method predicts that the hybridization of the dimethylaminophenyl nitrogen atom is more sp^3 than sp^2 in character, while experimentally the opposite is observed. For example, the Me–N–C–C dihedral angle in **2DA** is calculated to be 22.2°, whereas the angle is 5.84° in the X-ray structure.[20] The PM3 method thus strongly overestimates the dipole moment component along the *z*-axis; we assume it to be negligible. Likewise, calculated *z*-components of the hyperpolarizability will be exaggerated as well.

The presence of the dipole moment of the azomethine bridge determines that the calculated angle between the first hyperpolarizability and the dipole moments in **2D** and **3D** amounts to 45 and 56°, respectively. Hence, the vector components of β along the dipole moment β_μ, being measured by EFISH, are considerably smaller than the actual hyperpolarizabilities and have to be corrected. The effect of the local azomethine dipole moment on the direction of the relatively large dipoles of nitro compounds **2A** and **3A** is less dramatic. Angles between total hyperpolarizabilities β_{tot} and μ are 18° (**2A**) and 12° (**3A**). Since the respective cosines of these angles, 0.95 and 0.98, are close to unity $\beta\mu$ is a good measure for β_{tot} and EFISH hyperpolarizabilities will reflect actual first hyperpolarizabilities satisfactorily. The same holds for the donor–acceptor substituted compounds, where the contribution of the azomethine dipole moment to the total dipole moment is small.

It must however be realized that the PM3 calculated dipole moments μ_g are rather poorly in line with experimental dipole moments. The data in Table 5 reveal that calculated (total) dipole moments μ_{calc} of Dπ compounds **1–4D** are systematically underestimated, whereas those of the π*A* **1–4A** compounds are

** Definitions of the various calculated hyperpolarizabilities are to be found in the Experimental section.

Table 6 EFISH hyperpolarizabilities of compounds **1**–**4D**, **1**–**4A** and **1**–**4DA**

	μ_g/D [a]	$\mu_g\,\beta/10^{-48}$ esu	$\mu_g\,\beta(0)/10^{-48}$ esu	$\beta(0)/10^{-30}$ esu [b]	$\beta_{tot}/10^{-30}$ esu [c]
1D	2.4	40.2	33.5	14	13.6
2D	2.7	21.6	17.6	8.5	10.7
3D	3.6	46.6	38.8	14	16.6
4D	3.2	69.7	54.0	17	14.4
1A	4.6	82.9	69.1	15	13.3
2A	4.2	37.4	31.4	7.5	6.9
3A	5.0	42.7	36.5	7.3	12.0
4A	4.5	52.0	44.1	9.8	7.2
1DA	7.4	554.1	413.5	56	37.5
2DA	6.9	416.7	304.2	44	28.0
3DA	8.6	390.1	304.8	35	36.8
4DA	8.2	681.7	476.7	58	30.2

[a] Ground state dipole moment taken from ref. 31. Dipole moments were measured in benzene at 25 °C; for all benzylideneanilines the temperature was not specified.[30] [b] Experimental static hyperpolarizability. [c] PM3 calculated total hyperpolarizability.

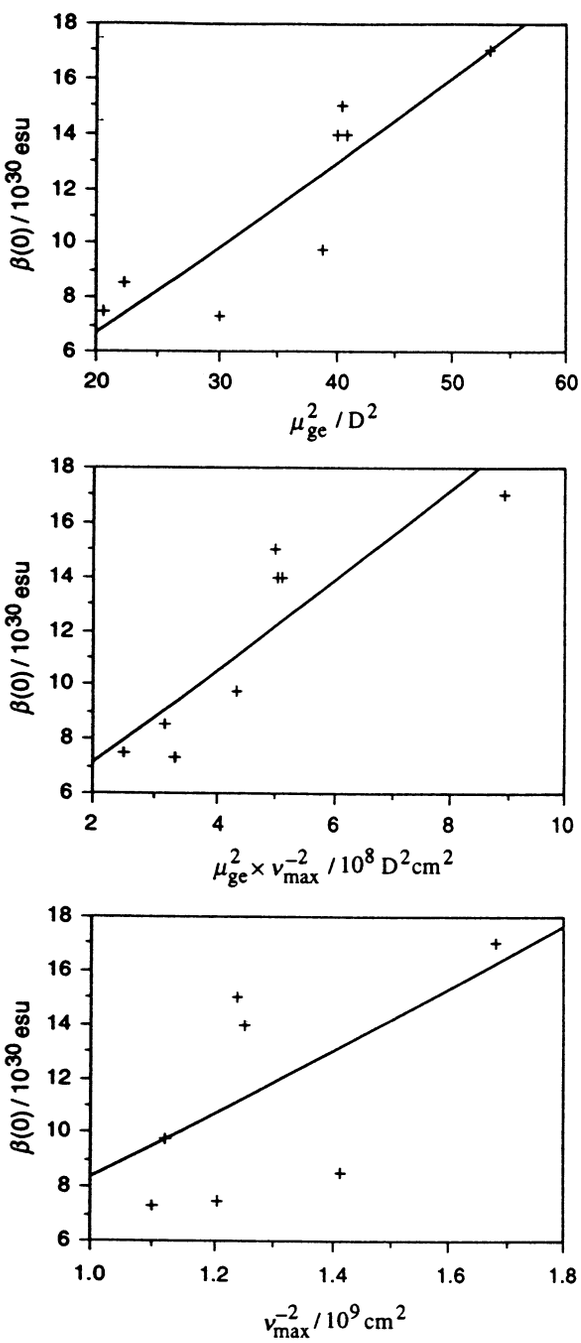

Fig. 4 Results of linear regression analysis between hyperpolarizabilities of all monosubstituted compounds and two-level model factors. Obtained relations are, with omission of exponents: $\beta(0) = 0.52 + 0.31\ \mu_{ge}^2$, $r = 0.890$, $\beta(0) = 3.83 + 1.67\ \mu_{ge}^2\ \nu_{max}^{-2}$, $r = 0.880$ and $\beta(0) = -3.14 + 1.15\ \nu_{max}^{-2}$, $r = 0.572$.

overestimated. Moreover, the calculated dipole moment of benzylideneaniline (**2**), and thus of the azomethine bridge, is too small as well. The consequence is that the actual angles between dipole moments and hyperpolarizabilities in **2A** and **3A** are larger than calculated, since the relative contribution of the bridge dipole moment, and hence μ_y, is larger. It is however plausible that these angles do not exceed 25° and that therefore β_μ is still a reasonable approximation for the actual β (cos 25 = 0.906). Concerning **2D** and **3D** the increase in going from the calculated to the experimental dipole moment is stronger than the increase found for **2**, suggesting that their dipole moments should be more aligned along the *x*-axis than calculated. As moreover the increase for **2D** is smaller than the increase for **3D** while the calculated angle for **3D** is larger we estimate θ in both compounds to be 40°. Thus, $\beta(0)$ of **2D** and **3D** (Table 6) is obtained upon dividing the $\mu_g\beta(0)$ data [by cos(40°) μ_g].

The EFISH results collected in Table 6 show that among the monosubstituted compounds hyperpolarizabilities $\beta(0)$ of the dimethylamino compounds are in general larger than those of the nitro compounds. Within each series the largest values are found for the azobenzene **4D** and the stilbene **1A**, respectively. In contrast, NLO activities of the monosubstituted benzylideneanilines are, with the exception of **3D**, rather small. PM3 calculated hyperpolarizabilities β_{tot} are in reasonable agreement with the experimental data.

The differences between the first hyperpolarizabilities of the monosubstituted compounds can be rationalized when they are analysed in terms of the two-level model. In Fig. 4, $\beta(0)$ is plotted *vs.* the factors which play a role in the two-level approximation, *i.e.* μ_{ge}^2, ν_{max}^{-2} and the product of these quantities, $\mu_{ge}^2\ \nu_{max}^{-2}$. Reliable $\Delta\mu$ data are unfortunately not available. Fig. 4 shows that upon plotting both $\beta(0)$ *vs.* μ_{ge}^2 (correlation coefficient *r* 0.890) and $\beta(0)$ *vs.* $\mu_{ge}^2\ \nu_{max}^{-2}$ ($r = 0.880$) a reasonable linear fit is obtained. In contrast, plotting of $\beta(0)$ *vs.* ν_{max}^{-2} yields a scatter plot. It is thus concluded that the transition dipole moment is the principal factor of interest for the nonlinear optical activities of the monosubstituted compounds. In the donor substituted series even an excellent linear relation between $\beta(0)$ and μ_{ge}^2 with a correlation coefficient of 0.997 is obtained. The transition energy appears to be less important, but still affects the hyperpolarizabilities since $\beta(0)$, μ_{ge}^2 and ν_{max}^{-2} are interrelated. The reason that β depends on μ_{ge} rather than on ν_{max} possibly is that there is a much greater variation in μ_{ge} than in ν_{max}. Differences in dipole moments $\Delta\mu$ must be of minor influence. It is expected that they are of similar magnitude for all compounds.

Hence, it appears that the relative low $\beta(0)$ of **2D** in comparison to the first hyperpolarizabilities of other donor compounds is caused by the low intensity of its absorption (Table 3). Whereas the transition energy of **2D** is more favourable than that of **3D** the smaller intensity renders the nonlinear optical response of **2D** considerably smaller. As stated above the small

Table 7 Additivity and CT contributions to the first hyperpolarizability[a]

	$\beta/10^{-30}$ esu	$\beta_{CT}/10^{-30}$ esu	$\beta_{add}/10^{-30}$ esu	$\beta_{add} + \beta_{CT}/10^{-30}$ esu	β_{CT}/β	β_{add}/β	$(\beta_{add} + \beta_{CT})/\beta$
1DA	56	38	29	67	0.68	0.52	1.20
2DA	44	33	16	49	0.75	0.48	1.11
3DA	35	31	21	52	0.89	0.68	1.67
4DA	58	51	27	78	0.88	0.47	1.34

[a] All hyperpolarizabilities in this Table are static hyperpolarizabilities.

transition intensity of **2D** is related to hampering of charge migration by the bridge. For the nitro compounds the high excitation energy of **3A** is less compensated by its transition intensity, resulting in comparable hyperpolarizabilities for **2A** and **3A**. The high $\beta(0)$ values of dimethylaminoazobenzene **4D** and nitrostilbene **1A** have their origin in a favourable combination of large transition dipoles and small transition energies. The optical nonlinearity of **4D** can be regarded as reflecting an appreciable CT interaction between the dimethylamino group and the azo bridge.

Among the donor–acceptor substituted compounds the largest first hyperpolarizabilities are found for stilbene **1DA** and azobenzene **4DA**, which are of comparable magnitude. The values for the benzylideneanilines are significantly smaller, $\beta(0)$ of **2DA** being the larger of the two. The hyperpolarizabilities of **1DA** and **2DA** are in line with data reported by Cheng *et al.*[6] (**1DA**: $\beta = 73 \times 10^{-30}$ esu at 1.91 μm in chloroform) and Singer *et al.*[15] (**1DA**: $\beta(0) = 52 \times 10^{-30}$ esu, **2DA**: $\beta(0) = 37 \times 10^{-30}$ esu, both in DMSO). The trend in increasing $\beta(0)$, **2DA** < **1DA** ≈ **4DA**, is also consistent with data given by Singer *et al.*,[15] which do not however include information on compounds of type **3**. Our experimental data however strongly contradict results of CNDO/S-CI calculations on 4-amino-4′-nitro substituted stilbene, azobenzene and benzylideneaniline systems by Tsunekawa and co-workers.[11,12] They reported that the nonlinear optical activity of **3DA** should be a factor of four to six less than those of the other compounds, for which unusual high values of 132 to 203 × 10^{-30} esu were predicted. Furthermore the calculated order of increasing β, **3DA** < **4DA** < **2DA** < **1DA**, differs from the sequence we found (**3DA** < **2DA** < **1DA** ≈ **4DA**). On the other hand, calculations by Morley[14] reproduce the magnitudes of and order in hyperpolarizabilities of **1**–**4DA** adequately. Our PM3 calculated hyperpolarizabilities provide a less satisfying picture. It is predicted that the nonlinear optical activities of **1DA** and **3DA** exceed those of **4DA** and **2DA**. Although the value obtained for **3DA** is overestimated since a planar geometry was used (30 × 10^{-30} esu is a more appropriate value[22]) trends in and magnitudes of the PM3 calculated hyperpolarizabilities do not fully correspond to the EFISH data.

According to Levine[45] and Oudar and Chemla[46] the first hyperpolarizability of a donor–acceptor substituted π-conjugated system is composed of an additive contribution β_{add}, which corresponds to a vector summation of hyperpolarizabilities of monosubstituted species and the CT contribution, eqn. (6), where usually $\beta_{CT} > \beta_{add}$.[45] Table 7 contains the

$$\beta = \beta_{add} + \beta_{CT} \quad (6)$$

additive and CT contributions to the total hyperpolarizabilities. Inspection of the data reveals that the CT contributions to the overall hyperpolarizability are large indeed; they range from 68 to 89%. Although $\beta(0)$ and $\beta_{CT}(0)$ are not linearly related, some positive correlation is present. Hence, to a first approximation differences in $\beta(0)$ can be rationalized by use of the two-level model. Linear correlations between $\beta(0)$ and two-level model factors are however not found. On the other hand, in a series of donor–acceptor compounds possessing an identical bridge often linear, albeit in some cases (double) logarithmic, relations between hyperpolarizabilities and transition energies are observed.[6,47] It appears that μ_{ge} in these series is relatively insensitive to the nature of the substituents and is primarily determined by the type of bridge, which rationalizes its minor impact on the hyperpolarizability. In the present case, where the bridge is varied, μ_{ge} and ν_{max} play an equally important role as $\Delta\mu$ is of comparable magnitude for all compounds. Consequently, the largest β is obtained for azobenzene **4DA**, which possesses both the largest transition intensity and the smallest excitation energy. Although in stilbene **1DA** a somewhat less favourable transition intensity and energy are combined, its first hyperpolarizability is hardly inferior to that of **4DA**. On the other hand the nonlinear optical activities of both benzylideneanilines are significantly smaller because the CT transition of **3DA** occurs at a relatively high wavenumber, while that of **2DA** possesses only a small transition dipole. The azomethine bridge thus provides a relative poor conjugation path. Its orientation dictates which two-level factor is affected in particular.

The information in Table 5 and Fig. 3 shows that within each compound type **1**–**4** the hyperpolarizabilities of the Dπ, πA, (Dπ + πA) and DπA systems are situated in more or less the same direction. Consequently, hyperpolarizabilities of Dπ and πA compounds can be added as scalar quantities to give β_{add} and be straightforwardly related to $\beta(0)$ data of DπA compounds. It is seen that additive hyperpolarizabilities of both benzylideneanilines are already inferior to those of the azobenzene and stilbene systems. Furthermore, β_{add} values contribute constantly to the total hyperpolarizability in the case of compound types **1**, **2** and **4**. The contribution of β_{add} for **3DA** is however significantly larger.

Summation of the β_{add} and β_{CT} data results in hyperpolarizabilities for the donor–acceptor compounds which are significantly larger than $\beta(0)$. The model described by eqn. (6), which proved to be successful in explaining hyperpolarizabilities of benzene derivatives,[45,46] seems thus not to be valid for stilbene-like compounds and provides too simplified a picture. Computational studies[5,48] have shown that more reliable results are obtained for these types of compounds by invoking a three-level rather than a two-level model. The former model takes, besides mixing of the ground (S_0) and CT states, mixing of the CT state and the second excited state (S_2) into account. The latter contribution to the overall hyperpolarizability is negative, and its magnitude is roughly proportional to the two-level term. Three-level terms may account for the observed discrepancies between the ($\beta_{add} + \beta_{CT}$) and $\beta(0)$ data. The largest three-level contributions are expected for **3DA** and **4DA**, the compounds for which the contribution of β_{CT} is most pronounced. For these two compounds the ratio $(\beta_{add} + \beta_{CT})/\beta(0)$ is the largest, indicating that three-level contributions are large indeed. The involvement of the S_2 state is also indicated by the PPP/SCF CI results, which show that the S_0–S_2 transition contributes to the CT bands. The importance of this transition is, however, difficult to assess.

Consequently, a detailed insight into the nonlinear optical properties of the donor–acceptor compounds is complicated as a result of a large number of relevant factors, from which some are difficult to assess. Although β_{add} and β_{CT} data fail to produce the quantitative magnitudes of $\beta(0)$ they nevertheless provide a qualitative understanding of differences in $\beta(0)$.

Conclusions

The second-order nonlinear optical behaviour of the monosubstituted compounds is strongly affected by the redox properties of the bridge and interactions of the bridge with substituents. The redox behaviour and the interactions are to a large extent determined by the presence of nitrogen atoms in the bridge, which is particularly exemplified by the properties of the monosubstituted benzylideneanilines. For the stilbenes, extension of the π-system appears to be a factor of peculiar interest.

First, hyperpolarizabilities of the ethylene and azo bridged donor–acceptor compounds are of comparable magnitude, but substitution of one carbon by a nitrogen atom has a negative effect on the NLO activity. This can be traced back to the electronic properties of the benzylideneanilines, which are strongly related to the orientation of the azomethine bridge. When the azomethine nitrogen atom is linked to the dimethylaminophenyl moiety and the carbon atom is bonded to the nitrophenyl part the electron donating and accepting properties of the respective dimethylamino and nitro groups are enhanced, resulting in a red shifted but low intensity optical transition. In the alternative orientation a stronger delocalization of substituent effects over the π-system occurs, leading to a more intensive but high energy CT transition.

Experimental

Syntheses and measurements

Compounds **1**–**4**, **4D** and **4A** were commercially available. Synthesis of stilbenes **1D**, **1A** and **1DA**,[49,50] benzylideneanilines[51] **2D**, **2A**, **2DA**, **3D**, **3A** and **3DA** and azobenzene[52] **4DA** was carried out following literature procedures. During the syntheses and purification of benzylideneanilines all manipulations were performed in a dry nitrogen atmosphere and dried solvents were used in order to avoid possible hydrolysis. All compounds were purified by recrystallization and/or sublimation; their identity and purity were checked by ^{1}H and ^{13}C NMR spectroscopy, IR spectroscopy and thin layer chromatography (TLC).

UV–VIS spectra were recorded on a Cary 1 spectrophotometer. Fluorescence spectra were obtained using a Spex Fluorolog instrument. Solvents used were of spectrophotometric grade and were dried on molecular sieves before use. Dibutyl ether (Janssen, 99%) was distilled prior to use. Cyclic voltammetry was performed using an EG&G Model 273 potentiostat/galvanostat at a scan rate of 0.1 V s^{-1}. Solutions of 0.5 g l^{-1} in acetonitrile (Janssen p.A. grade, dried on 3 Å molecular sieves) were used in the presence of 0.1 M tetrabutylammonium hexafluorophosphate (Fluka, electrochemical grade) as supporting electrolyte. Redox potentials were measured relative to the $Ag/AgNO_3$ (0.01 M) system and were converted into values relative to standard calomel electrode (SCE) by measuring the oxidation potential of the $FeCp/FeCp^{\cdot+}$ couple ($E_{\frac{1}{2}}$ *vs.* SCE = 0.31 V[53]) in the system.

The experimental approach used for the EFISH measurements[41,54] is essentially identical to those described by Levine and Bethea[55] and Oudar.[56] Solutions in chloroform in a wedge-shaped cell were irradiated with 1.5 mJ pulses of a Raman shifted (1907 nm) output of an injection seeded Nd:YAG laser. A quartz crystal ($d_{11} = 1.04 \times 10^9$ esu) was used as reference sample. The magnitude of the applied static electric field was 5×10^7 V m^{-1}. The reproducibility of the measurements was within 10% and the experimental error *ca.* 15%. Measured hyperpolarizabilities were corrected for dispersion to yield static hyperpolarizabilities $\beta(0)$ using eqn. (7), where $\beta(\omega)$ is the

$$\beta(0) = \beta(\omega)\frac{(\omega_{max}^2 - 4\omega^2)(\omega_{max}^2 - \omega^2)}{\omega_{max}^4} \qquad (7)$$

hyperpolarizability at the fundamental frequency ω (1.572×10^{14} s^{-1}) and ω_{max} is the frequency at the absorption maximum of the NLO chromophore.

Calculations

PPP/SCF/CI calculations, including a full CI treatment, were performed using Griffiths' program[25,26] on planar molecular geometries. Calculations of hyperpolarizabilities were carried out within the finite field approximation such as implemented in the MOPAC package,[43,44] using the PM3 method.[57] Molecular geometries were first fully optimized using the same semi-empirical method; calculated structures all were essentially planar. The precise option was used as convergence criterion for calculations on both geometries and nonlinear optical properties. Vector components of calculated hyperpolarizabilities were obtained from eqn. (8), and the total hyperpolarizability β_{tot}

$$\beta_i = \tfrac{3}{5}\sum_j \beta_{ijj} \qquad (8)$$

from eqn. (9). The vector component of β along the dipole moment direction, β_μ, was obtained using eqn. (10).

$$\beta_{tot} = (\beta_x^2 + \beta_y^2 + \beta_z^2)^{\frac{1}{2}} \qquad (9)$$

$$\beta_\mu = \frac{\beta_{tot}\,\mu}{||\mu||} = \sum_{i=x}^{z}\frac{\beta_i\,\mu_i}{||\mu||} \qquad (10)$$

Given β values are those derived from the effect of the applied electric field on the heat of formation, since these values are less sensitive to the convergence of the SCF than the dipole expansion data.[58] Nevertheless, hyperpolarizabilities obtained from the energy and dipole expansions were always in good mutual accordance, indicative of a good precision of the calculations. Otherwise than prescribed[43] calculated hyperpolarizabilities were not divided by 2.0 since a zero frequency electric field was used.[58] All calculations were run on a 486/33 MHz personal computer.

References

1 P. N. Prasad and D. J. Williams, *Introduction to Nonlinear Optical Effects*, in *Molecules and Polymers*, Wiley, New York, 1991.
2 D. J. Williams, *Angew. Chem.*, 1984, **96**, 637.
3 D. F. Eaton, *Science*, 1991, **253**, 281.
4 S. R. Marder and J. W. Perry, *Adv. Mater.*, 1993, **5**, 804.
5 D. R. Kanis, M. A. Ratner and T. J. Marks, *Chem. Rev.*, 1994, **94**, 195.
6 L.-T. Cheng, W. Tam, S. H. Stevenson, G. R. Meredith, G. Rikken and S. R. Marder, *J. Phys. Chem.*, 1991, **95**, 10 631.
7 L.-T. Cheng, W. Tam, S. R. Marder, A. E. Stiegman, G. Rikken and C. W. Spangler, *J. Phys. Chem.*, 1991, **95**, 10 643.
8 S. R. Marder, D. N. Beratan and L.-T. Cheng, *Science*, 1991, **252**, 103.
9 S. R. Marder, L.-T. Cheng, B. G. Tiemann, A. C. Friedli, M. Blanchard-Desce, J. W. Perry and J. Skindøj, *Science*, 1994, **263**, 511.
10 S. M. Risser, D. N. Beratan and S. R. Marder, *J. Am. Chem. Soc.*, 1993, **115**, 7719.
11 T. Tsunekawa, T. Gotoh and M. Iwamoto, *Chem. Phys. Lett.*, 1990, **166**, 353.
12 T. Tsunekawa, T. Gotoh, H. Mataki, T. Kondoh, S. Fukuda and M. Iwamoto, *Proc. SPIE*, 1990, **1337**, 272.
13 T. Tsunekawa and K. Yamaguchi, *J. Phys. Chem.*, 1992, **96**, 10 268.
14 J. O. Morley, *J. Chem. Soc., Perkin Trans. 2*, 1995, 731.
15 K. D. Singer, J. E. Sohn, L. A. King, H. M. Gordon, H. E. Katz and C. W. Dirk, *J. Opt. Soc. Am. B*, 1989, **6**, 1339.
16 R. Akaba, K. Tokamaru and T. Kobayashi, *Bull. Chem. Soc. Jpn.*, 1980, **53**, 1993.
17 R. Akaba, H. Sakuragi and K. Tokumaru, *Bull. Chem. Soc. Jpn.*, 1985, **58**, 1711.
18 R. Akaba, H. Sakuragi and K. Tokumaru, *Bull. Chem. Soc. Jpn.*, 1985, **58**, 1186.
19 E. Haselbach and E. Heilbronner, *Helv. Chim. Acta*, 1968, **51**, 16.

20 H. Nakai, M. Shiro, K. Ezumi, S. Sakata and T. Kubota, *Acta Crystallogr., Sect. B*, 1976, **32**, 1827.
21 L. N. Patnaik and S. Das, *Bull. Chem. Soc. Jpn.*, 1987, **60**, 4421.
22 C. A. van Walree, A. W. Maarsman, A. W. Marsman, M. C. Flipse, W. J. J. Smeets, A. L. Spek and L. W. Jenneskens, *J. Chem. Soc., Perkin. Trans. 2*, following paper.
23 M. H. Charlton, R. Docherty, D. J. McGeein and J. O. Morley, *J. Chem. Soc., Faraday Trans.*, 1993, **89**, 1671.
24 J. O. Morley, *J. Mol. Struct.* (*Theochem*), 1995, **340**, 45.
25 J. Griffiths and J. G. Lasch, QCPE program QCMP054.
26 J. Griffiths, *Dyes and Pigments*, 1982, **3**, 211.
27 H. H. Jaffé and M. Orchin, *Theory and Applications of Ultraviolet Spectroscopy*, Wiley, New York, 1962, p. 276.
28 A. J. Duben, *J. Chem. Educ.*, 1985, **62**, 373.
29 M. El-Aasser, F. Abdel-Halim and M. A. El-Bayoumi, *J. Am. Chem. Soc.*, 1971, **93**, 590.
30 E. Hertel and M. Schinzel, *Z. Physik. Chem.*, 1941, **B48**, 289.
31 A. L. McClellan, *Tables of Experimental Dipole Moments*, Freeman, San Francisco, 1963.
32 R. Pariser and R. G. Parr, *J. Chem. Phys.*, 1953, **21**, 767.
33 P. Skrabal, J. Steiger and H. Zollinger, *Helv. Chim. Acta*, 1975, **58**, 800.
34 E. Lippert, *Z. Elektrochem.*, 1957, **61**, 962.
35 C. Reichardt, *Solvents and Solvent Effects in Organic Chemistry*, VCH, Weinheim, 2nd edn., 1988.
36 R. Hermant, Ph.D. Thesis, University of Amsterdam, 1990.
37 W. Liptay, in *Excited States*, ed. E. C. Lin, Academic Press, New York, 1974, vol. 1, p. 129.
38 E. G. McRae, *J. Phys. Chem.*, 1957, **61**, 562.
39 M. S. Paley, J. M. Harris, H. Looser, J. C. Baumert, G. C. Bjorklund, D. Jundt and R. J. Twieg, *J. Org. Chem.*, 1989, **54**, 3774.
40 M. Belletête, B. Scheuer-Lamalle, L. Baril and G. Durocher, *Can. J. Spectrosc.*, 1977, **22**, 31.
41 M. C. Flipse, R. de Jonge, R. H. Woudenberg, A. W. Marsman, C. A. van Walree and L. W. Jenneskens, *Chem. Phys. Lett.*, 1995, **245**, 297.
42 M. C. Flipse, R. de Jonge, R. H. Woudenberg, A. W. Marsman, C. A. van Walree and L. W. Jenneskens, *Proc. Org. Thin Films for Photonics Applications Topical Meeting, OSA Annual Meeting*, Portland, Oregon, 1995; *Technical Digest Series*, 1995, **21**, 374.
43 J. J. P. Stewart, MOPAC, version 6.0, QCPE program 504, 1990.
44 H. A. Kurtz, J. J. P. Stewart and K. M. Dieter, *J. Comput. Chem.*, 1990, **11**, 82.
45 B. F. Levine, *Chem. Phys. Lett.*, 1976, **37**, 516.
46 J. L. Oudar and D. S. Chemla, *J. Chem. Phys.*, 1977, **66**, 2664.
47 A. E. Stiegman, E. Graham, K. J. Perry, L. R. Khundkar, L.-T. Cheng and J. W. Perry, *J. Am. Chem. Soc.*, 1991, **113**, 7658.
48 D. R. Kanis, M. A. Ratner and T. J. Marks, *J. Am. Chem. Soc.*, 1992, **114**, 10 338.
49 G. Riezebos and E. E. Havinga, *Recl. Trav. Chim. Pays-Bas*, 1961, **80**, 446.
50 P. Pfeiffer, *Ber.*, 1915, **48**, 1777.
51 *Organikum*, VEB, Berlin, 1981, p. 481.
52 R. Meldola, *J. Chem. Soc.*, 1884, **45**, 107.
53 J. Dachbach, D. Blackwood, J. W. Pons and S. Pons, *J. Electroanal. Chem.*, 1987, **237**, 269.
54 R. A. Huijts and G. L. J. Hesselink, *Chem. Phys. Lett.*, 1989, **156**, 209.
55 B. F. Levine and C. G. Bethea, *J. Chem. Phys.*, 1975, **63**, 2666.
56 J. L. Oudar, *J. Chem. Phys.*, 1977, **67**, 446.
57 J. J. P. Stewart, *J. Comput. Chem.*, 1989, **10**, 209.
58 N. Matsuzawa and D. A. Dixon, *J. Phys. Chem.*, 1992, **96**, 6232.

Paper 6/04603G
Received 2*nd July* 1996
Accepted 19*th Novermber* 1996